



Deposited via The University of Leeds.

White Rose Research Online URL for this paper:

<https://eprints.whiterose.ac.uk/id/eprint/199964/>

Version: Accepted Version

Article:

Ding, H, Nili, A, Chen, J et al. (2023) Effects of cold storage temperature on thermoreversible aging in heavily oxidized asphalt binders. *Construction and Building Materials*, 389. 131792. ISSN: 0950-0618

<https://doi.org/10.1016/j.conbuildmat.2023.131792>

© 2023 Elsevier Ltd. All rights reserved. © 2022, Elsevier. This manuscript version is made available under the CC-BY-NC-ND 4.0 license <http://creativecommons.org/licenses/by-nc-nd/4.0/>.

Reuse

This article is distributed under the terms of the Creative Commons Attribution-NonCommercial-NoDerivs (CC BY-NC-ND) licence. This licence only allows you to download this work and share it with others as long as you credit the authors, but you can't change the article in any way or use it commercially. More information and the full terms of the licence here: <https://creativecommons.org/licenses/>

Takedown

If you consider content in White Rose Research Online to be in breach of UK law, please notify us by emailing eprints@whiterose.ac.uk including the URL of the record and the reason for the withdrawal request.

1 **Effects of cold storage temperature on thermoreversible aging in heavily**
2 **oxidized asphalt binders**

3 Haibo Ding^{a,b}, Azuo Nili^{a,b}, Jiale Chen^c, Zonghao Yang^{a,b*}, Hadis Jemal
4 Muktar^{a,b}, David Connolly^d, Yanjun Qiu^{a,b}

5 haibo.ding@swjtu.edu.cn; azuo.nili@my.swjtu.edu.cn; cn20jc2@leeds.ac.uk;
6 yangzonghao@my.swjtu.edu.cn; hadismuktar@my.swjtu.edu.cn; Dconnolly@leeds.ac.uk;
7 yanjunqiu. @swjtu.edu.cn

8 ^aSchool of Civil Engineering, Southwest Jiaotong University, Chengdu Sichuan 610031, China.

9 ^bHighway Engineering Key Laboratory of Sichuan Province, Southwest Jiaotong University,
10 Chengdu, Sichuan 610031, China.

11 ^cSWJTU-Leeds Joint School, Southwest Jiaotong University, Chengdu, Sichuan 610031,
12 China.

13 ^dSchool of Civil Engineering, University of Leeds, Leeds LS2 9JT, UK

14 *Corresponding author: yangzonghao@my.swjtu.edu.cn (Zonghao Yang)

15 **Abstract**

16 In order to better understand the thermoreversible aging characteristics of asphalt after heavy oxidation, six
17 selected heavily oxidized asphalt containing different proportions of C₂₀H₄₂ are subjected to extended
18 bending beam rheometer (ExBBR) tests, while modulated differential scanning calorimetry (MDSC) and
19 atomic force microscope (AFM) are also performed on the asphalt. The results indicate that the introduction
20 of heavy oxidation will not only affect the low temperature properties of the asphalt but also its
21 thermoreversible aging characteristics, but this effect will receive an influence of the storage temperature.

22 This is due to the increase in viscosity of the asphalt after heavy oxidation, which makes it difficult for
23 $C_{20}H_{42}$ to migrate, while the increase in storage temperature can release the potential of the degree of
24 thermoreversible aging of the asphalt by accelerating the movement of wax molecules. And like $C_{20}H_{42}$, the
25 grade loss of asphalt blended with $C_{30}H_{62}$ is different at different storage temperatures and oxidation levels,
26 which proves that for heavily oxidized asphalt, multiple storage temperatures should be selected for testing
27 its grade loss. Combined with thermal and morphological analysis, the introduction of heavy oxidation not
28 only increases the amount of wax precipitation, but also significantly increases the thermoreversible aging
29 of the asphalt by lowering the T_g of the asphalt and forming more perfect crystals during low temperature
30 storage. Finally, by comparing the grade loss due to cold storage and extended oxidation, it can be found that
31 the incorporation of $C_{20}H_{42}$ will make the asphalt more influenced to physical hardening. Therefore, it is
32 necessary to study the effect of asphalt wax content on the degree of thermoreversible aging of heavily
33 oxidized asphalt.

34 **Keywords:** Asphalt binder; Thermoreversible aging; Crystalline wax; Oxidative aging; Physical hardening

35 **1. Introduction**

36 Petroleum asphalt is one of the most widely used materials in pavement construction
37 owing to its good bonding and waterproofing properties. Because of its unique characteristics
38 such as excellent waterproofing, high damping ratio, good integrity, asphalt has also been
39 utilized in other applications such as water conservancy, railway engineering. Countries such
40 as the United States, Germany, Japan, and China has carried out a large number of studies on
41 asphalt concrete subgrade [1, 2]. Compared with other ordinary subgrade, the advantages of

42 asphalt concrete subgrade mainly include the following five aspects: (1) reducing the stress
43 effect of upper loads on the subgrade and transferring them to the lower structure; (2) keeping
44 the moisture content of the subgrade stable as an impermeable layer; (3) acting as a support
45 layer for ballast and reducing ballast splash; (4) alleviating train vibration and reducing noise;
46 (5) reducing the whole life cycle cost of the track structure due to the reduction of later
47 maintenance [3, 4]. The authors' team has systematically studied the damage pattern of full-
48 section railway asphalt concrete subgrade and found that when asphalt concrete is positioned
49 at a lower level in the railway subgrade, the train loads tend to be smaller, thus determined that
50 thermal shrinkage cracks become an important factor affecting the durability of asphalt
51 concrete [5, 6]. Among the many influencing factors, thermoreversible aging could affect
52 asphalt concrete subgrade performance in the long run [7-9]. One of the main reasons is that
53 other forms of aging mainly occur on the pavement surface while thermoreversible aging
54 occurs in the whole asphalt pavement structure, especially in cold areas.

55 In order to understand the mechanism of thermoreversible aging as an important basis for
56 the production of high-quality asphalt and solving related pavement distresses, in recent years
57 researchers have devoted themselves to explain the causes of physical hardening in asphalt.
58 The term physical hardening was first introduced by Anderson from Shell Laboratories,
59 Amsterdam, The Netherlands, who attributed the phenomenon to the precipitation of waxes
60 and the aggregation of asphaltenes, noting that both processes are very slow at low temperature
61 [10]. Some asphalt will form large microcrystalline wax crystals during long-term low-
62 temperature storage and are affected by the change of pavement temperature. Therefore,

63 different asphalt could have different allowable wax contents, which is also the reason why
64 wax is considered to be the main factor in thermoreversible aging [11, 12]. In contrast, studies
65 have shown that waxes in asphalt are a mixture of alkanes, cycloalkanes and aromatic
66 compounds and dominated by n-alkanes with carbon numbers of $C_{15}\sim C_{57}$ [13]. Kavinichi found
67 that although $C_{20}H_{42}$ can promote the physical hardening in asphalt, this tendency is affected
68 by the base asphalt binder and is not determined by the content of $C_{20}H_{42}$ solely [14].
69 Subsequent studies found that not all waxes will aggravate the thermoreversible aging of
70 asphalt. Compared with $C_{20}H_{42}$, $C_{30}H_{62}$ is significantly less effective in promoting the physical
71 hardening of asphalt, while squalanecan improve the low temperature performance of asphalt
72 without aggravating the degree of thermoreversible aging [15, 16].

73 Despite a number of studies have conducted a series of studies on the effects of waxes
74 with different numbers of carbon molecules on the thermoreversible aging behaviour of asphalt,
75 the low temperature performance and grade loss of asphalt in most of these studies are
76 measured after a PAV-20h test using the standard BBR procedure [15, 17, 18]. In recent years
77 some practitioners have questioned this conventional PAV aging method, as Simon's research
78 has shown that the PAV-20h test is only able to simulate the condition of asphalt pavements
79 after 5-6 years of use, which is clearly not suitable to reflect the field aging of the pavement
80 surface after a long term service [19]. In order to be able to simulate the long-term use of
81 asphalt pavement, Simon proposed to prolong the aging time of PAV test in another study to
82 prepare heavily oxidized asphalt, and found that the asphalt under a PAV-40h test can simulate
83 the condition of asphalt pavements after 10-15 years of use [20]. Other researchers have

84 explored the low-temperature performance distribution of different asphalts after extended
85 aging. Kilger's research shows that the effect of recycling oils, including bio-oil and REOB,
86 on the improvement of asphalt's low-temperature performance tends to be weakened after
87 heavy oxidation compared with asphalt without recycling oils [21]. Ma, on the other hand,
88 found that the degree of thermoreversible aging of recycled asphalt blended with three different
89 rejuvenators can only be distinguished after RTFO and PAV aging, and increases with the
90 extension of PAV aging time [22]. This indicates that like the low-temperature properties of
91 asphalt, the degrees of thermoreversible aging of different asphalts after severe oxidation will
92 also be different, and thus it is necessary to investigate the mechanism of the effect of waxes
93 on the physical hardening properties of heavily oxidized asphalt binders.

94 In view of this, the purpose of this paper is to investigate the interaction between
95 thermoreversible aging and irreversible aging based on extended bending beam rheometer
96 (ExBBR) tests, using six different asphalt samples blended with pure wax, and analyzing the
97 grade loss of heavily oxidized asphalt by introducing three different aging methods, RTFO,
98 PAV-20h, and PAV-40h test. Based on the results of ExBBR tests, modulated differential
99 scanning calorimetry (MDSC) and atomic force microscopy (AFM) were used to analyze the
100 mechanism of the effect of wax on the physical hardening properties of heavily oxidized asphalt.

101 **2. Experimental program**

102 **2.1. Materials**

103 **2.1.1 Asphalt binder**

104 According to research, the wax content of asphalt will affect the road performance of
105 asphalt pavement. In this paper, six kinds of asphalt from different crude oils were selected,
106 among which the base asphalt from Venezuela came from the Strategic Highway Research
107 Program (SHRP) Material Reference Library (MRL), which is labeled as ABG, according to
108 the research there is basically no wax in ABG [23]. While the other asphalt samples are used
109 for comparison, which are labeled as SWE, CAL, MAO, UNK, and ZNH, whose source and
110 performance grade (PG) are shown in Table 1. The first three kinds of asphalt binders are
111 commonly used in other countries while the rest of the asphalt binders usually used in asphalt
112 pavement construction in China. To compare the oxidative aging with thermoreversible aging,
113 in this research, the asphalt binders are tested after going through the rolling thin film oven
114 (RTFO) as well as 20h and 40h of pressure aging vessel (PAV) tests.

115 **Table 1.** Basic properties of asphalt binders.

Sample Code	Source	Limiting high temperature	Limiting low temperature
		PG (°C)	PG (°C)
ABG	Venezuela	65.2	-29.7
SWE	Sweden	63.8	-31.3

CAL	Caltex, Korea	67.1	-26.5
MAO	Maoming, China	64.9	-28.6
UNK	Unknown, China	65.7	-29.5
ZHH	Zhonghai, China	66.3	-27.7

116 **2.1.2 Additives**

117 According to previous research on wax in asphalt [15], the waxes in asphalt are mainly
118 composed of saturated straight-chain hydrocarbons. Since waxes are an important cause of
119 thermoreversible ageing of asphalt. Therefore, two commercial n-alkanes produced by Sigma-
120 Aldrich were chosen as pure wax additives in this study, namely n-eicosane ($C_{20}H_{42}$) and n-
121 dodecane ($C_{32}H_{66}$), with a purity of 99%. Considering that most asphalts for paving have a wax
122 content of less than 7% [24-26], the percent of wax additives were blended at 1%, 3%, 5% and
123 7% by mass of asphalt binder. To ensure that the wax can be uniformly distributed in the asphalt,
124 the base asphalt binder is heated to 165°C during the mixing process and the prepared model
125 asphalt is sheared for 1h using a shear mixer.

126 **2.2. Test Methods**

127 **2.2.1 Extended bending beam rheometer (ExBBR)**

128 Among different low-temperature evaluation methods developed for asphalt binder in
129 recent years [27, 28], the most mature and widely used one is the bending beam rheometer
130 (BBR) test to measure the low temperature performance grade (PG) of asphalt binders.

131 However, it has also been shown that asphalt pavement designed based on PG performance
132 suffered from severe low-temperature cracking from time to time [29], due to the increase in
133 stiffness of asphalt binders at low temperatures with increasing storage time [30, 31]. Based on
134 this, the ExBBR test was developed. Compared to the regular BBR test, the ExBBR test
135 requires testing the PG performance of the asphalt in six states (3 conditioning time×2 storage
136 temperature) separately. The grade loss obtained from the ExBBR test can be used to evaluate
137 the degree of thermoreversible aging of asphalt. According to the requirements of AASHTO
138 TP122-17, the grade loss of asphalt should be less than 6°C.

139 2.2.2 *Modulated differential scanning calorimetry (MDSC)*

140 To understand the thermoreversible aging process of asphalt binders throughout the
141 service temperature range, the MDSC test was chosen for the study to analyze the thermal
142 behavior of asphalt. In contrast to conventional thermal analysis tests, the MDSC test allows
143 the total heat flow signal to be divided into reversing and non-reversing heat flow signals,
144 which has been favored by many researchers [32, 33]. The procedure is as follows. First, the
145 sample is heated to 120°C and then left at this temperature for 10min so that to melt all the
146 crystal structures. Second, the specimen is cooled down to 80°C at a cooling rate of 20°C/min
147 to avoid overrate oxidation and saving time. Next, the sample is rapidly cooled to -90°C at
148 10°C/min and kept for 10min. Then, the asphalt sample is heated to 120°C at a heating rate of
149 600°C/h (10°C/min). Finally, the total heat flow, reversing heat flow, non-reversing heat flow
150 and the first derivative of reversing heat flow are employed as the four key parameters to
151 characterize the thermal behavior of asphalt binder.

152 2.2.3 Atomic force microscope (AFM)

153 As a visco-elastic-plastic material with significant temperature dependence, asphalt has
154 been the subject of many studies on the formation and growth mechanisms of the ‘bee-like’
155 structure in the AFM microstructure parameters. It has been shown that the ‘bee-like’ structure
156 can be explained based on the wax nucleation theory, leading to the conclusion that its
157 morphological characteristics are related to the heating history, cooling rate and aging degree
158 of the sample [34-36]. As this study is focused on the differences in the microscopic
159 morphology of different asphalts after low-temperature storage, the asphalt is stored at low
160 temperature for 72h, and the surface of the asphalt is tested in amplitude mode using an AFM
161 probe. In order to ensure the repeatability of the observation results, three replicates were
162 carried out for each asphalt sample.

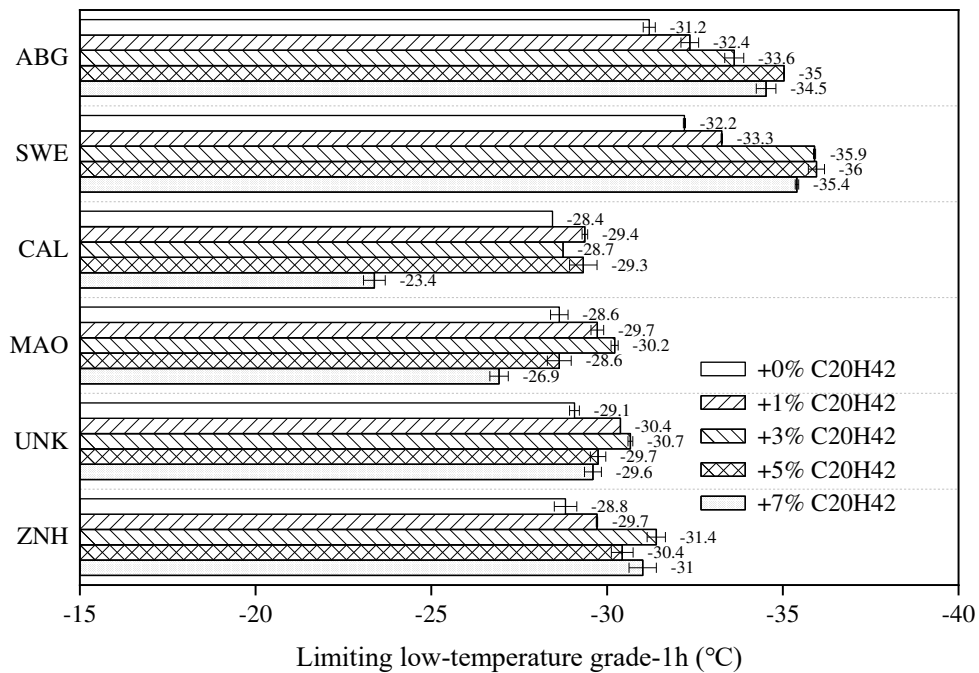
163 3. Results and discussion

164 3.1 Oxidation effects on limiting grade of asphalt binder

165 Fig. 1 shows the oxidation effects on limiting grade of asphalt binder based on ExBBR
166 test. As can be seen, the addition of $C_{20}H_{42}$ to different RTFO aged asphalts effectively
167 decreased the limiting grade of asphalt in the beginning. In fact, the addition of 5% of $C_{20}H_{42}$
168 to ABG and SWE exhibited the best improvement in terms of low-temperature performance
169 (limiting grade was reduced by $4^{\circ}C$), followed by MAO, UNK and ZNH (limiting grade was
170 reduced by $1^{\circ}C\sim 2^{\circ}C$) while CAL had the least improvement (limiting grade was reduced by
171 less than $1^{\circ}C$). However, the limiting grade of most asphalts began to increase after adding 3%

172 of C₂₀H₄₂ while for ABG and SWE the turning point was at 5%. Combined with previous
 173 research results [37, 38], this may be due to the different wax contents of asphalts from different
 174 origins which asphalt with low wax content can accommodate more C₂₀H₄₂ before saturation.

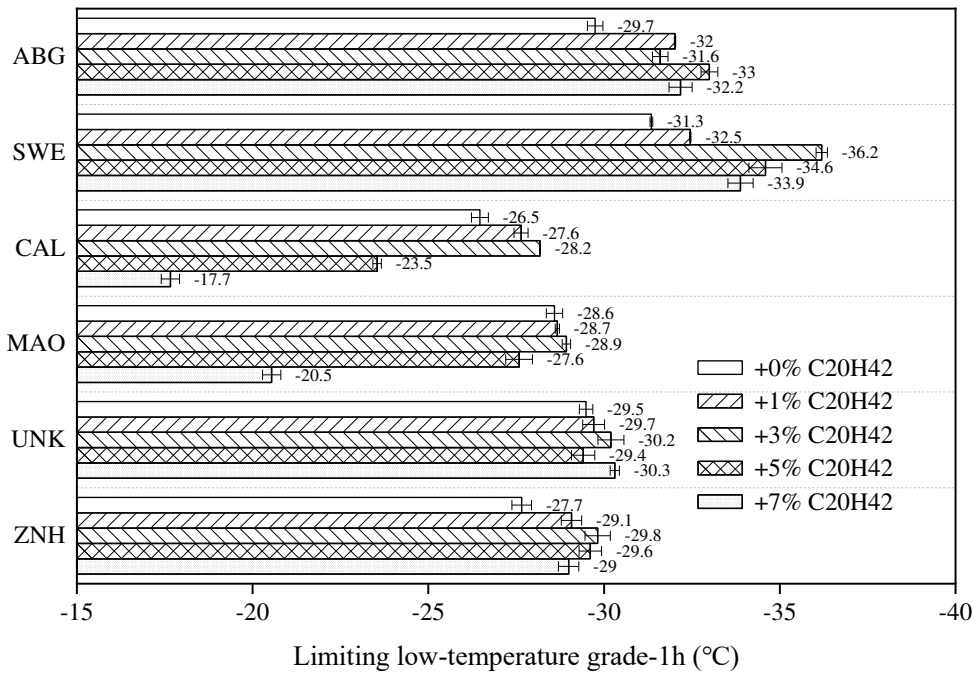
175 By comparing the limiting grade of asphalt at different aging stages: 40h PAV>20h
 176 PAV>RTFO, for most asphalts compared to RTFO the limiting grade of asphalt after 40h PAV
 177 has increased by 1°C~2°C. Meanwhile, it is worth noting that the limiting grade of ABG and
 178 SWE after 40h PAV starts to increase with more than 3% of C₂₀H₄₂, which indicates that the
 179 introduction of heavy oxidation will not only lead to the deterioration of asphalt low
 180 temperature performance, but also lead to the decrease in the capacity for n-alkanes in asphalt.



181

182

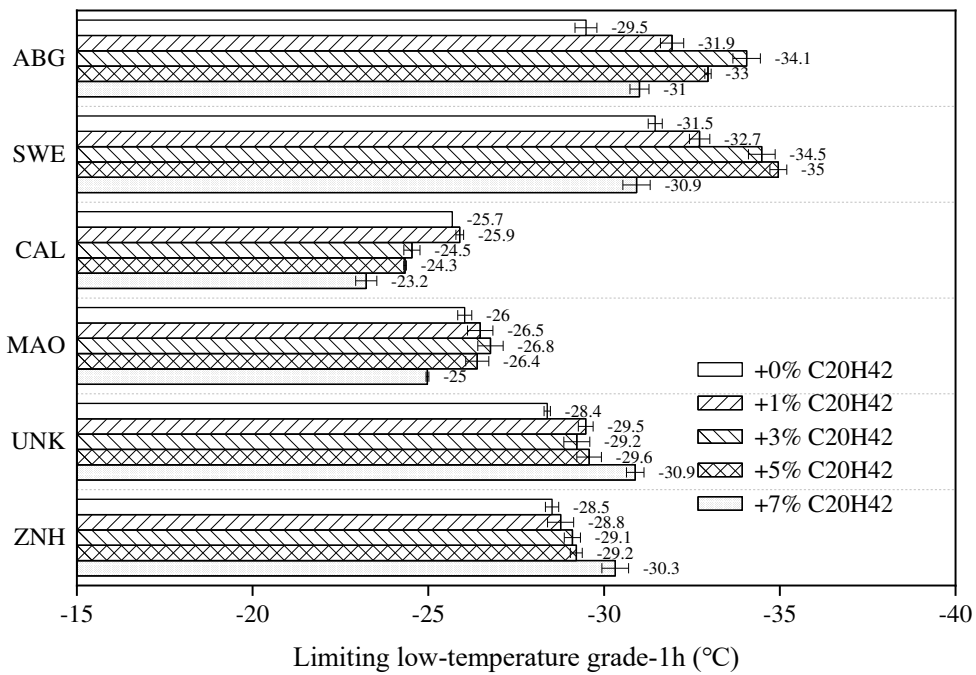
(a) RTFO



183

184

(b) 20h PAV



185

186

(c) 40h PAV

187

Fig. 1. Oxidation effects on limiting grade of asphalt binder.

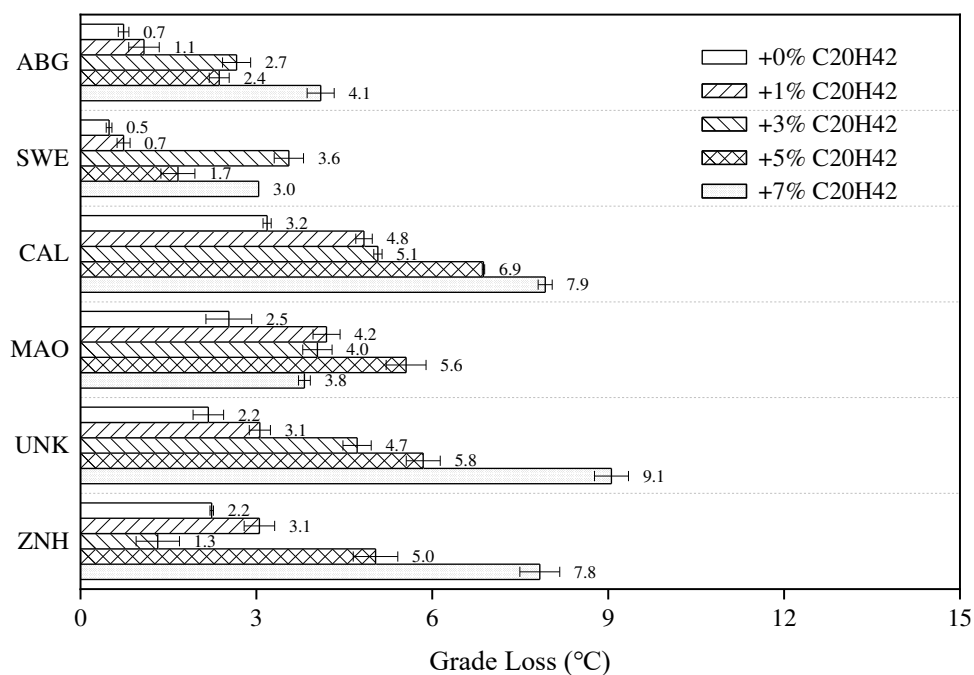
188 *3.2 Oxidation effects on grade loss of asphalt binder*

189 If only based on the limiting grade of the asphalt binder, it can be easily concluded that
190 for most asphalt the addition of $C_{20}H_{42}$ is an effective solution to improve the low temperature
191 performance of asphalt and that this improvement is almost independent of the effects of
192 oxidative aging. However, some studies in recent years have shown that with the extension of
193 the storage time of asphalt in low-temperature environment, the wax and asphaltene in the
194 asphalt begin to slowly aggregate and exhibit physical hardening, which indirectly affects the
195 low-temperature performance of the asphalt [25, 39].

196 According to the result of grade loss of asphalt blended with $C_{20}H_{42}$ in low temperature
197 environment given in Fig. 2, it can be observed that there is no significant difference in the
198 grade loss of six asphalt without wax in RTFO aging stage, while the grade loss of six asphalt
199 after blending with $C_{20}H_{42}$ can be easily distinguished. Among the six asphalt, CAL, MAO,
200 UNK and ZNH blended with high content of $C_{20}H_{42}$ all showed significant hardening behavior
201 with grade loss higher than $6^{\circ}C$. In contrast, the degree of thermoreversible aging of ABG and
202 SWE, on the other hand, is not significantly affected by n-alkanes, and the maximum grade
203 loss is only about $4^{\circ}C$. Referring to the research of Ding [23], this is due to the fact that ABG
204 contains almost no wax and thus the asphalt can accommodate more wax before saturation.

205 Compared to the RTFO aging stage, the grade loss of most asphalt has increased after
206 PAV. However, for ABG and SWE blended with $C_{20}H_{42}$, the grade loss of asphalt after 20h
207 PAV remained almost unchanged. In contrast, after the introduction of 40h PAV, the grade loss

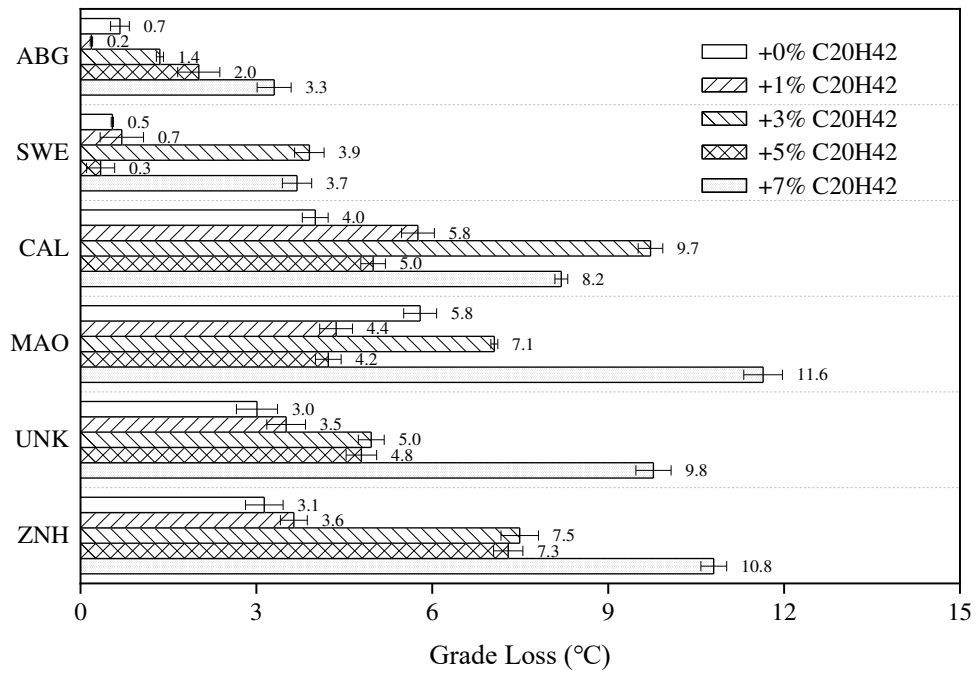
208 of the above two asphalt after heavy oxidation has increased to around 6°C. This can be
 209 explained using the findings of Tabatabaee [40, 41], that is, the presence of waxes will promote
 210 the phase separation of asphaltene components in asphalt. As the degree of oxidation increases,
 211 the increase of asphaltene content in asphalt will accelerate the rate of phase separation,
 212 resulting in a rapid increase in the hardening tendency of asphalt. However, this theory is not
 213 sufficient to explain the effect of the thermo-oxidative aging on the degree of thermoreversible
 214 aging of the other four types of asphalt. Taking MAO+3% C₂₀H₄₂ as an example, the grade loss
 215 of asphalt at the 20h PAV and 40h PAV stages is 7.1°C and 7.6°C, respectively. While for
 216 UNK+3% C₂₀H₄₂, the grade loss of heavily oxidized asphalt decreased from 5.0°C at the 20h
 217 PAV stage to 3.2°C at the 40h PAV stage.



218

219

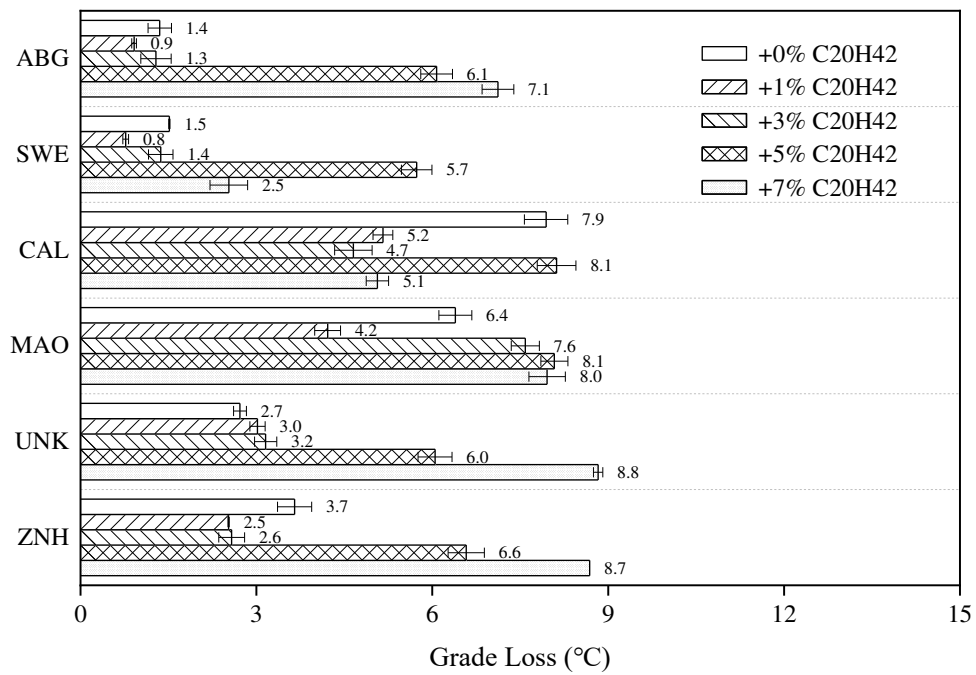
(a) RTFO



220

221

(b) 20h PAV



222

223

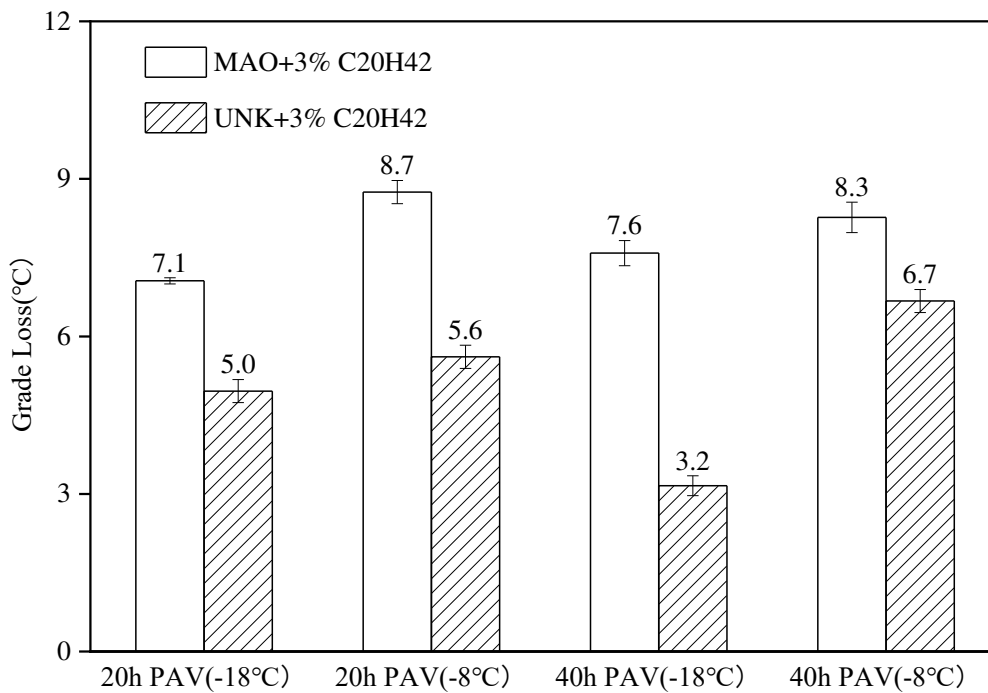
(c) 40h PAV

224

Fig. 2. Oxidation effects on grade loss of asphalt binder.

225 **3.3 Storage temperature effects on grade loss of asphalt binder**

226 To further explain the effect of heavy oxidation on the grade loss of MAO+3% C₂₀H₄₂
227 and UNK+3% C₂₀H₄₂, this study chose -8°C as the control group based on the original storage
228 temperature (-18°C) to investigate the effect of storage temperature on the grade loss of heavily
229 oxidized asphalt, as shown in Fig. 3. It can be seen from the figure that when the storage
230 temperature is increased from -18°C to -8°C, the grade loss of asphalt also shows an increasing
231 tendency. But for the two different asphalt, the increase in grade loss differs. For MAO+3%
232 C₂₀H₄₂, the degree of thermoreversible aging of the asphalt after 20h PAV and 40h PAV
233 remains almost the same after increasing the storage temperature, whereas the difference in
234 grade loss between each is only 0.4°C. As for UNK+3% C₂₀H₄₂, the increase in storage
235 temperature unleashed the potential for the degree of thermoreversible aging of heavily
236 oxidized asphalt, and at a storage temperature of -8°C, the grade loss of asphalt after 40h PAV
237 increased by 3.5°C, surpassing the sample after 20h PAV.



238

239

Fig. 3. Grade loss of asphalt binders under different cold storage temperature.

240

Such phenomenon can be explained according to the phase separation theory [42-45],

241

according to which asphalt can be viewed as a binary mixture consisting of bitumen and wax,

242

a typical binary mixture is shown in Fig. 4. As can be seen in the figure, the distribution states

243

of the phases of the asphalt differ at different temperatures. When the temperature is high

244

enough (T_1), the mixture is stable at any binary ratio. And as the temperature decreases, the

245

mixture may go through a metastable state (T_2) and eventually reach an unstable state (T_3).

246

After entering the metastable state or even the unstable state, the wax phase in the asphalt starts

247

to separate from the asphalt phase, causing the aggregation of wax molecules and eventually

248

leading to the crystalline precipitation of wax in the asphalt. Combined with the findings of Lei

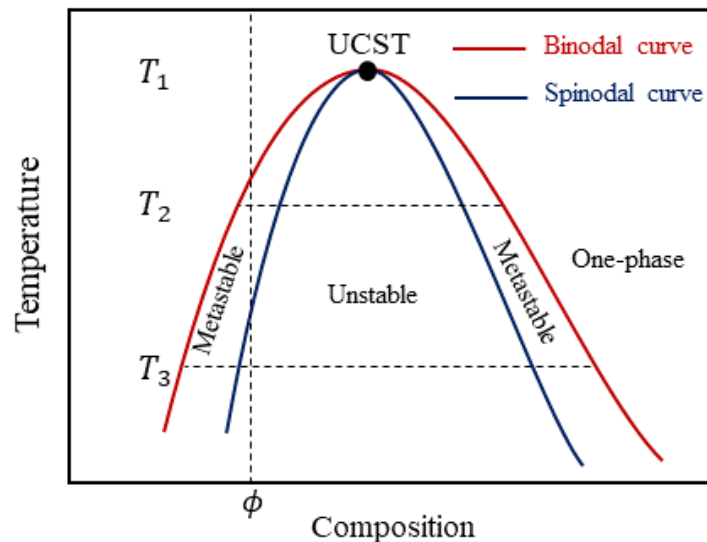
249

[46], it can be explained that the viscosity of asphalt increases after heavy oxidation, which

250

makes it difficult for wax molecules to migrate and thus inhibits wax precipitation. Therefore,

251 even if heavily oxidized asphalt has reached an unstable state in a low temperature environment,
252 there may not be significant thermoreversible aging inside the asphalt. In this case, the increase
253 in storage temperature will effectively accelerate the movement rate of wax molecules, and the
254 degree of thermoreversible aging of asphalt will be increased.

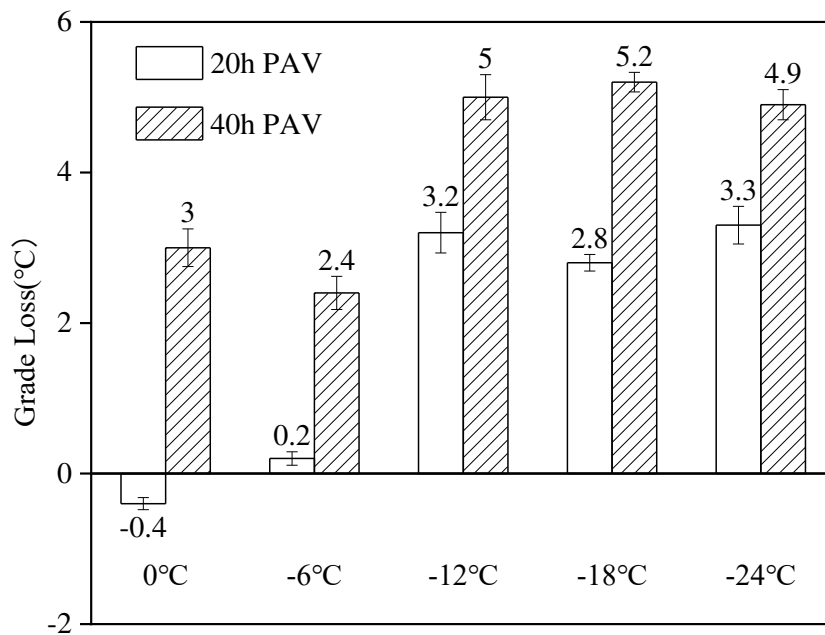


255

256 **Fig. 4.** Possible phase diagram of the asphalt at different temperature.

257 In order to be able to confirm whether the storage temperature will affect the precipitation
258 and crystallization of n-alkanes other than $C_{20}H_{42}$ in asphalt. In this study, ABG with almost no
259 wax is selected as the base asphalt, and $C_{30}H_{62}$ is used as the additive to study the effect of
260 storage temperature on the grade loss of PAV aged ABG+5% $C_{30}H_{62}$, and the results are shown
261 in Fig. 5. As shown in the figure, if only following the traditional test method, the grade loss
262 of oxidized asphalt ($-18^{\circ}C$, 20h PAV) is $2.8^{\circ}C$. By changing the storage temperature and
263 oxidation degree of the tested asphalt, the grade loss is only $-0.4^{\circ}C$ under the optimal storage
264 conditions ($0^{\circ}C$, 20h PAV), while the grade loss of asphalt increased to $5.2^{\circ}C$ under the worst
265 storage conditions ($-18^{\circ}C$, 40h PAV). This indicates that, like $C_{20}H_{42}$, the effect of $C_{30}H_{62}$ on

266 the degree of thermoreversible aging of asphalt is quite different at different storage
 267 temperatures and oxidation degrees. Therefore, in order to better characterize the
 268 thermoreversible aging of heavily oxidized asphalt, multiple storage temperatures should be
 269 selected to test the grade loss of the asphalt.



270

271

Fig. 5. Grade loss of ABG+5%C30 caused by isothermal conditioning.

272

3.4 Influence mechanism of oxidative aging on physical hardening of asphalt binder

273

274

275

276

277

278

In order to further explain the influence mechanism of oxidative aging on the physical hardening of asphalt, two aging stages of ABG+5% C₂₀H₄₂ are selected for the study, RTFO and 40h PAV, with a grade loss of 2.4°C and 6.1°C, respectively, and MDSC is used to investigate the thermal behavior of ABG+5% C₂₀H₄₂ at different oxidative aging stages, as shown in Fig. 6. Based on the non-reversing heat flow curves of the asphalt, it can be seen that there is an endothermic peak in the asphalt at both aging stages, while the area of the

279 endothermic peak reflects the amount of crystal fraction (CF) in the asphalt, which is usually
280 caused by the crystallization or precipitation of long-chain alkane compounds [47, 48].
281 Compared with RTFO, the temperature corresponding to the endothermic peak of asphalt after
282 40h PAV decreased from 9.6°C to -6.0°C, with an area increase of 12.3%. As for the reversing
283 heat flow of asphalt, significant difference in the shape of the DSC curves of asphalt at different
284 aging stages can be observed, indicating that phase separation occurs in asphalt after heavy
285 oxidation. The first derivative of reversing heat flow curves of the asphalt at the RTFO and 40h
286 PAV aging stages have an maximum value at 28.3°C and 9.5°C, respectively, which can be
287 regarded as the glass transition temperature (T_g) of the asphalt [9]. The decrease of T_g of asphalt
288 after heavy oxidation will lead to a larger proportion of $C_{20}H_{42}$ in high-elastic state in the early
289 cooling stage, and this part of $C_{20}H_{42}$ will be changed from high-elastic state to glassy state
290 with higher molecular chain stiffness after long-term low-temperature storage. This means that
291 the heavy oxidation will not only cause more waxes to crystallize out of the asphalt, but will
292 also significantly aggravate the degree of thermoreversible aging of the asphalt by lowering the
293 T_g of the asphalt to a more perfect crystal during low temperature storage.

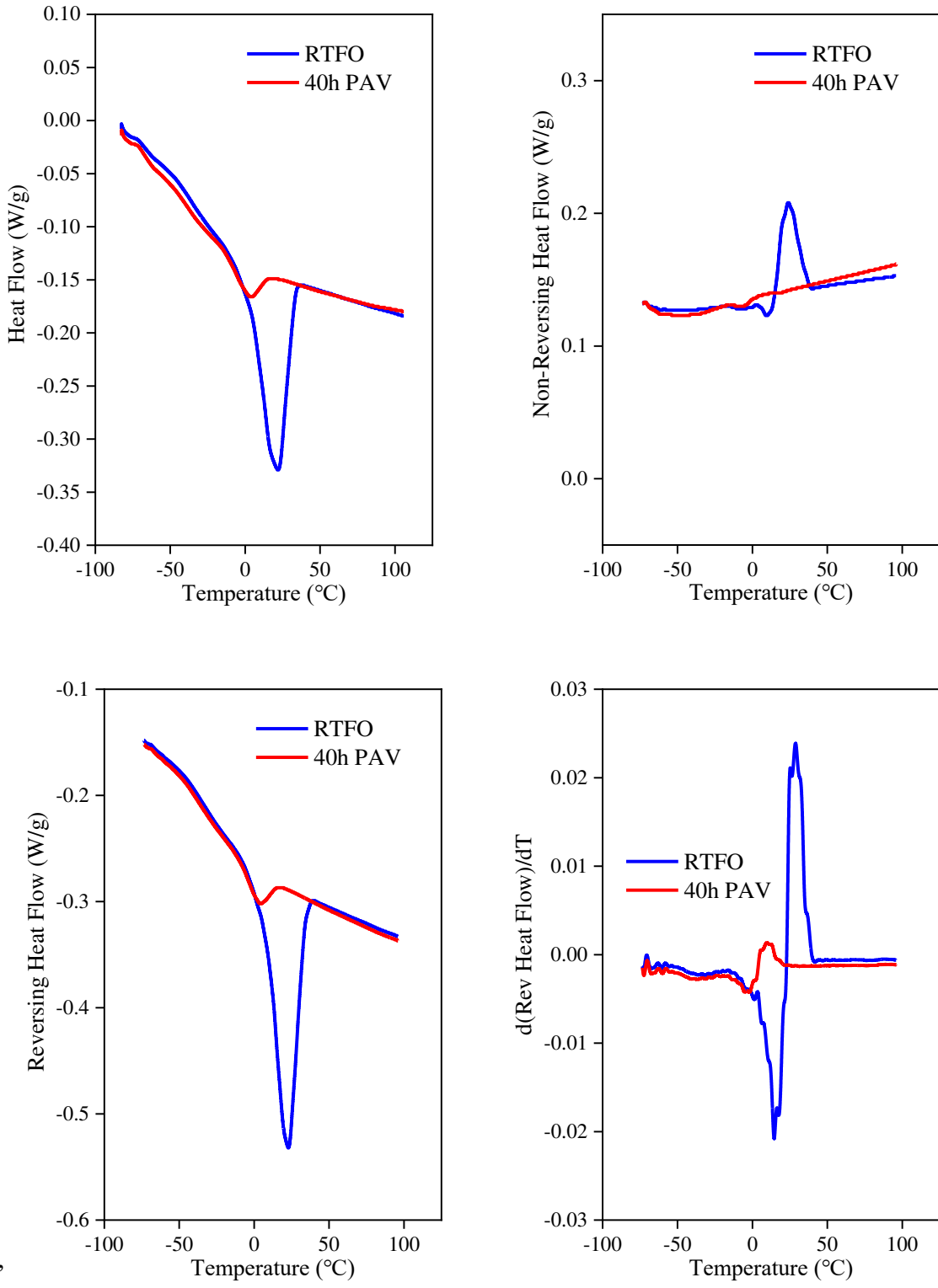
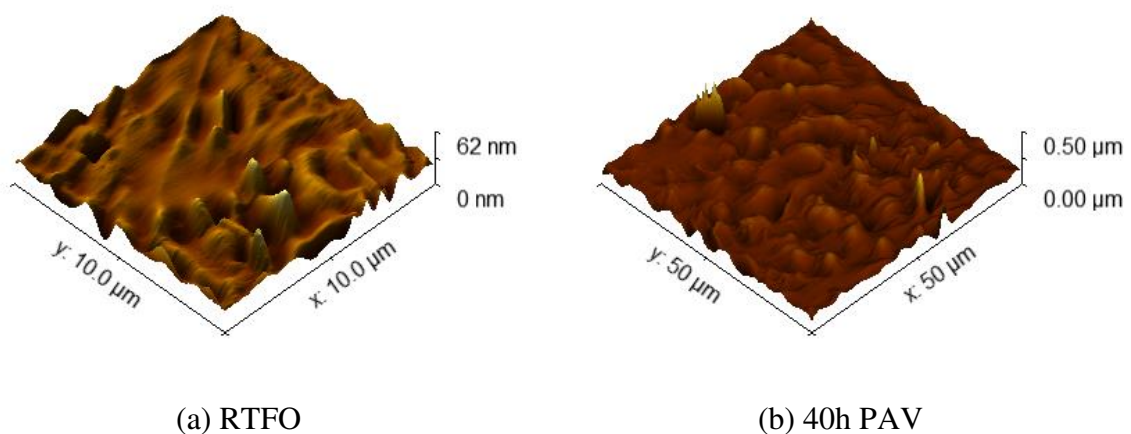


Fig. 6. Thermal behavior of ABG+5% C₂₀H₄₂ under different oxidation degree.

295 And the surface micromorphology images of ABG+5% C₂₀H₄₂ under two different aging
296 states in AFM amplitude mode are shown in Fig. 7. From Fig. 7, it can be seen that there are a
297 large number of peaks like protrusions on the asphalt surface after RTFO, while the number of
298 peaks on the surface increases after 40h PAV and its peak value also grows to 0.5μm. Such
299 peak like protrusion is related to the crystallization of microcrystalline wax and waxy
300 molecules when cooled to the test temperature [49]. To quantitatively evaluate the effect of
301 peak like protrusions on the surface morphology of the asphalt, the average roughness (R_a) and
302 root mean square roughness (R_q) are calculated by Gwyddion software to describe the
303 roughness of asphalt, the values of which are shown in Table 2. The results show that after
304 heavy oxidation, the R_a and R_q of the asphalt increased by 5.58 mm and 8.28 nm, respectively,
305 indicating that the increase in oxidation degree will lead to an increase in the surface roughness
306 of asphalt, that is, more wax will precipitate from asphalt crystals, leading to an increase in the
307 degree of thermoreversible aging of asphalt.



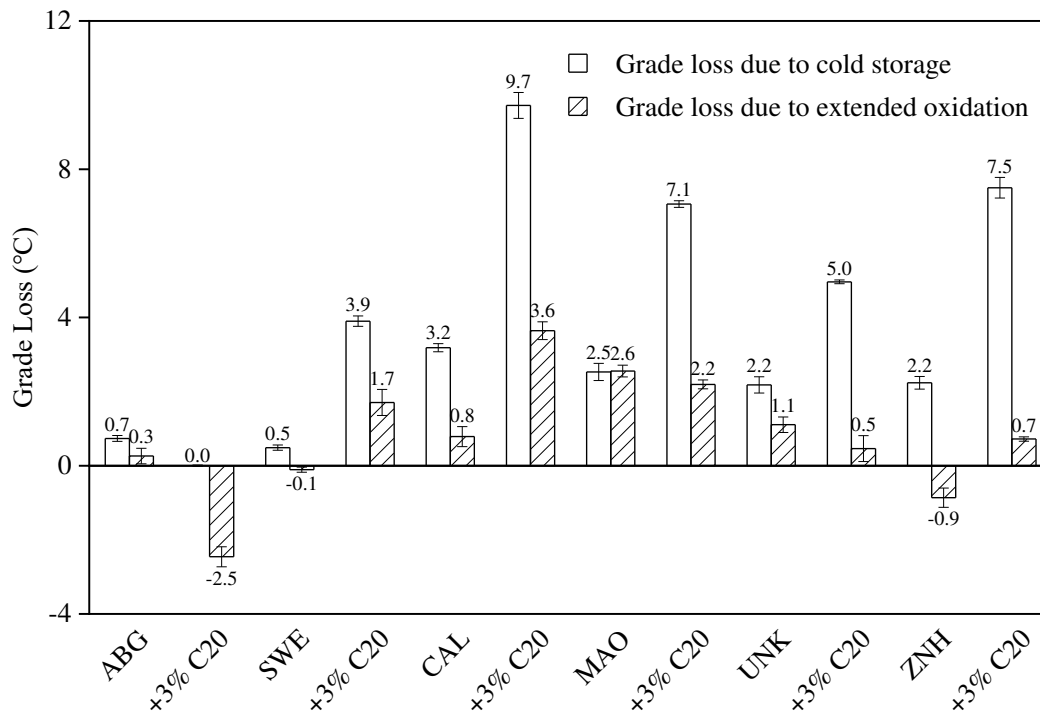
308 **Fig. 7.** AFM images of ABG+5% C₂₀H₄₂ under different oxidation degree.

309 **Table 2.** Surface roughness statistics of ABG+5% C₂₀H₄₂.

Oxidation degree	R_a (nm)	R_q (nm)
RTFO	10.68	15.17
40h PAV	16.26	23.38

310 **3.5 Comparison between thermoreversible aging and oxidation**

311 Fig. 8 compares the grade loss due to cold storage and extended oxidation. As shown, for
312 most of the asphalts, physical hardening has a stronger impact on grade loss than oxidation.
313 For the asphalt samples not blended with n-alkanes, there is no significant dominance of
314 physical hardening on grade loss, and the difference between the two is less than half a 3°C. In
315 contrast, with asphalt blended with C₂₀H₄₂, the grade loss due to cold storage increased
316 significantly, and the grade loss gap caused by cold storage and extended aging grew to 6°C,
317 which indicates that the grade loss of wax-blended asphalt is determined by physical hardening.
318 Therefore, it is necessary to study the effect of asphalt wax content on the degree of
319 thermoreversible aging of heavily oxidized asphalt.



320

321

Fig. 8. Grade loss of asphalt binder due to cold storage and extended oxidation.

322

4. Conclusions

323

In this paper, the effects of cold storage temperature on the thermoreversible aging characteristics of asphalt binder samples doped with wax additives, especially heavily oxidized asphalts, were studied through a series of laboratory experiments. The following conclusions can be drawn from the results:

327

(1) With the appropriate addition of $C_{20}H_{42}$, the limiting grade of asphalt can be reduced,

328

while due to the different sources of asphalt crude oil, some asphalt with lower wax content

329

can accommodate more n-alkanes. While the introduction of heavy oxidation will not only lead

330

to the deterioration of asphalt low temperature performance, but also lead to the decrease in the

331

capacity for n-alkanes in asphalt.

332 (2) Among the six asphalt binders, for ABG and SWE blended with $C_{20}H_{42}$, the maximum
333 grade loss of both asphalt binders was only about $4^{\circ}C$ during the RTFO stage due to the
334 extremely low wax content, while the grade loss of asphalt after 20h PAV was almost
335 unchanged. However, after 40h PAV, the grade loss of asphalt grows to $6^{\circ}C$, which indicates
336 that asphalt with good grade loss under low aging conditions may also show significant
337 thermoreversible aging behavior after heavy oxidation.

338 (3) For the $C_{20}H_{42}$ -doped asphalt with high viscosity, there is a tendency to decrease the
339 grade loss of asphalt in low temperature storage after heavy oxidation instead. This is due to
340 the viscosity of asphalt increases after heavy oxidation, which makes it difficult for wax
341 molecules to migrate, thus inhibiting the precipitation of wax. In this case, the increase in
342 storage temperature will effectively accelerate the movement of wax molecules, thus releasing
343 the potential of the degree of thermoreversible aging of heavily oxidized asphalt.

344 (4) Similar to $C_{20}H_{42}$, for heavy oxidized asphalt blended with $C_{30}H_{62}$, the effect of $C_{30}H_{62}$
345 on the degree of thermoreversible aging of asphalt is quite different at different storage
346 temperatures and oxidation levels, and the grade loss distribution of asphalt varies from $-0.4^{\circ}C$
347 to $5.2^{\circ}C$. Therefore, in order to better characterize the thermoreversible aging of heavily
348 oxidized asphalt, multiple storage temperatures should be selected to test the grade loss of
349 asphalt.

350 (5) The results of MDSC and AFM show that heavy oxidation will not only cause more
351 wax to crystallize out of the asphalt, which leads to an increase in surface roughness, but also

352 significantly increases the thermoreversible aging of the asphalt by lowering the T_g of the
353 asphalt and forming more perfect crystals during low temperature storage.

354 (6) By comparing the grade loss due to cold storage and extended oxidation, it can be
355 observed that for most asphalt, physical hardening has a stronger impact on grade loss than
356 oxidation. Especially for asphalt blended with $C_{20}H_{42}$, the grade loss gap caused by cold storage
357 and extended oxidation grows from 3°C to 6°C. Therefore, it is necessary to study the effect of
358 asphalt wax content on the degree of thermoreversible aging of heavily oxidized asphalt.

359 **Acknowledgements**

360 This study was supported by the Interdisciplinary Cultivation Fund of SWJTU under Grant
361 No.YH15001124322147, National & Local Joint Engineering Research Center of
362 Transportation and Civil Engineering Materials (Chongqing Jiaotong University), National
363 Natural Science Foundation of China under Grant No.52008352 and 52178438, Sichuan
364 Science and Technology Program under Grant No. 2023NSFSC0022, and the Royal Society
365 (IEC\NSFC\211306 - International Exchanges 2021 Cost Share). The authors appreciate the
366 Analysis and Testing Center of Southwest Jiaotong University for their assistance on the AFM
367 and DSC tests.

368 **Reference**

- 369 [1] S.-H. Lee, Y.-T. Choi, H.-M. Lee, D.-W. Park, Performance evaluation of directly fastened
370 asphalt track using a full-scale test, *Construction and Building Materials* 113 (2016) 404-414.
371 [2] X. Zhong, X. Zeng, J. Rose, Shear modulus and damping ratio of rubber-modified asphalt

372 mixes and unsaturated subgrade soils, *Journal of Materials in Civil Engineering* 14(6) (2002)
373 496-502.

374 [3] K. Jadidi, M. Esmaeili, M. Kalantari, M. Khalili, M. Karakouzian, A review of different
375 aspects of applying asphalt and bituminous mixes under a railway track, *Materials* 14(1) (2020)
376 169.

377 [4] X. Xiao, D. Cai, L. Lou, Y. Shi, F. Xiao, Application of asphalt based materials in railway
378 systems: A review, *Construction and Building Materials* 304 (2021) 124630.

379 [5] M. Fang, Y. Qiu, C. Ai, Y. Wei, Gradation determination of impermeable asphalt mix on
380 subgrade surface layer for ballastless track in high-speed railway lines, *ICTE 2011* 2011, pp.
381 1926-1931.

382 [6] M. Fang, Y. Qiu, J.G. Rose, R.C. West, C. Ai, Comparative analysis on dynamic behavior
383 of two HMA railway substructures, *Journal of Modern Transportation* 19(1) (2011) 26-34.

384 [7] M. Berkowitz, M. Filipovich, A. Baldi, S.A. Hesp, J.P. Aguiar-Moya, L.G. Loría-Salazar,
385 Oxidative and thermoreversible aging effects on performance-based rheological properties of
386 six Latin American asphalt binders, *Energy & Fuels* 33(4) (2019) 2604-2613.

387 [8] H. Ding, A. Nili, A. Rahman, C. Yan, Y. Qiu, D. Connolly, Role of asphalt binder
388 compositions in the thermoreversible aging Process, *International Journal of Pavement*
389 *Engineering* (2022) 1-9.

390 [9] Y. Qiu, H. Ding, P. Zheng, Toward a better understanding of the low-temperature reversible
391 aging phenomenon in asphalt binder, *International Journal of Pavement Engineering* 23(2)
392 (2022) 240-249.

393 [10] D.A. Anderson, D.W. Christensen, H.U. Bahia, R. Dongre, M. Sharma, C.E. Antle, J.
394 Button, Binder characterization and evaluation, volume 3: Physical characterization, Asphalt
395 Cement 3 (1994).

396 [11] L.C. Michon, D.A. Netzel, T.F. Turner, D. Martin, J.-P. Planche, A ¹³C NMR and DSC
397 study of the amorphous and crystalline phases in asphalts, Energy & Fuels 13(3) (1999) 602-
398 610.

399 [12] S. Zherebtsov, A. Moiseev, Composition of the wax fraction of bitumen from methylated
400 brown coals, Solid Fuel Chemistry 43(2) (2009) 71-79.

401 [13] X. Lu, P. Redelius, Compositional and structural characterization of waxes isolated from
402 bitumens, Energy & Fuels 20(2) (2006) 653-660.

403 [14] J. Kovinich, S.A. Hesp, H. Ding, Modulated differential scanning calorimetry study of
404 wax-doped asphalt binders, Thermochemica Acta 699 (2021) 178894.

405 [15] H. Ding, H. Zhang, H. Liu, Y. Qiu, Thermoreversible aging in model asphalt binders,
406 Construction and Building Materials 303 (2021) 124355.

407 [16] H. Ding, H. Zhang, X. Zheng, C. Zhang, Characterisation of crystalline wax in asphalt
408 binder by X-ray diffraction, Road Materials and Pavement Design (2022) 1-17.

409 [17] H. Ding, H. Liu, Y. Qiu, A. Rahman, Effects of crystalline wax and asphaltene on
410 thermoreversible aging of asphalt binder, International Journal of Pavement Engineering (2021)
411 1-10.

412 [18] H. Liu, Q. Xie, H. Ding, H. Zhang, Y. Qiu, Rheological properties of model wax doped
413 asphalt binders, Construction and Building Materials 350 (2022) 128865.

- 414 [19] E.I. Ahmed, S.A. Hesp, S.K.P. Samy, S.D. Rubab, G. Warburton, Effect of warm mix
415 additives and dispersants on asphalt rheological, aging, and failure properties, *Construction*
416 *and Building Materials* 37 (2012) 493-498.
- 417 [20] J. Erskine, S. Hesp, F. Kaveh, Another look at accelerated aging of asphalt cements in the
418 pressure aging vessel, *Proceedings, Fifth Eurasphalt and Eurobitumen Congress, Istanbul,*
419 *Turkey, 2012.*
- 420 [21] A. Kilger, D. Swiertz, H.U. Bahia, Long-term aging performance analysis of oil modified
421 asphalt binders, *Transportation Research Record* 2673(12) (2019) 404-412.
- 422 [22] J. Ma, Y. Deng, D. Sun, S.A. Hesp, Relationship between thermoreversible and irreversible
423 aging in rejuvenated asphalt binder, *Construction and Building Materials* 358 (2022) 129463.
- 424 [23] H. Ding, H. Zhang, H. Zhang, Y. Qiu, Direct Observation of Crystalline Wax in Asphalt
425 Binders by Variable-temperature Polarizing Microscope, *Journal of Materials in Civil*
426 *Engineering* 34(10) (2022) 04022244.
- 427 [24] H.H. Kim, K.-D. Jeong, M.S. Lee, S.-J. Lee, Effect of ft paraffin wax contents on
428 performance properties of crumb rubber–modified asphalt binders, *Journal of Materials in Civil*
429 *Engineering* 27(11) (2015) 04015011.
- 430 [25] J. Kovinich, A. Kuhn, A. Wong, H. Ding, S.A. Hesp, Wax in Asphalt: A comprehensive
431 literature review, *Construction and Building Materials* 342 (2022) 128011.
- 432 [26] P. Romero, J. Youtcheff, K. Stuart, Low-temperature physical hardening of hot-mix asphalt,
433 *Transportation Research Record* 1661(1) (1999) 22-26.
- 434 [27] H. Ding, Y. Qiu, A. Rahman, Influence of thermal history on the intermediate and low-

435 temperature reversible aging properties of asphalt binders, *Road Materials and Pavement*
436 *Design* 21(8) (2020) 2126-2142.

437 [28] Y.J. Qiu, H.B. Ding, A. Rahman, H.Y. Luo, Application of dispersant to slow down
438 physical hardening process in asphalt binder, *Materials and Structures* 52(1) (2019).

439 [29] M. Ou Zhao, S.A. Hesp, Performance grading of the Lamont, Alberta C-SHRP pavement
440 trial binders, *International Journal of Pavement Engineering* 7(3) (2006) 199-211.

441 [30] H. Ding, S.A. Hesp, Variable-temperature Fourier-transform infrared spectroscopy study
442 of asphalt binders from the SHRP Materials Reference Library, *Fuel* 298 (2021) 120819.

443 [31] H.A. Tabatabaee, R. Velasquez, H.U. Bahia, Predicting low temperature physical
444 hardening in asphalt binders, *Construction and Building Materials* 34 (2012) 162-169.

445 [32] H. Ding, Y. Qiu, A. Rahman, Low-temperature reversible aging properties of selected
446 asphalt binders based on thermal analysis, *Journal of Materials in Civil Engineering* 31(3)
447 (2019) 04018402.

448 [33] P. Kriz, J. Stastna, L. Zanzotto, Temperature dependence and thermo-reversibility of
449 physical hardening of asphalt binders, 4th Eurasphalt & Eurobitume Congress, Copenhagen,
450 Denmark, 2008.

451 [34] A.M. Hung, E.H. Fini, AFM study of asphalt binder “bee” structures: Origin, mechanical
452 fracture, topological evolution, and experimental artifacts, *Rsc Advances* 5(117) (2015) 96972-
453 96982.

454 [35] J. Ji, Z. Suo, R. Zhang, H. Li, B. Han, J. Wang, Z. You, Effect of physical hardening on
455 low temperature performance of DCLR modified asphalt, *Construction and Building Materials*

456 295 (2021) 123545.

457 [36] H.H. Kim, M. Mazumder, A. Torres, S.-J. Lee, M.-S. Lee, Characterization of CRM
458 binders with wax additives using an atomic force microscopy (AFM) and an optical microscopy,
459 *Advances in Civil Engineering Materials* 6(1) (2017) 504-525.

460 [37] H. Ding, S.A. Hesp, Variable-temperature Fourier-transform infrared spectroscopy study
461 of wax precipitation and melting in Canadian and Venezuelan asphalt binders, *Construction
462 and Building Materials* 264 (2020) 120212.

463 [38] H. Ding, S.A. Hesp, Quantification of crystalline wax in asphalt binders using variable-
464 temperature Fourier-transform infrared spectroscopy, *Fuel* 277 (2020) 118220.

465 [39] Y.J. Qiu, H.B. Ding, A. Rahman, E.H. Yang, Using combined Avrami-Ozawa method to
466 evaluate low-temperature reversible aging in asphalt binders, *Road Materials and Pavement
467 Design* 21(1) (2020) 78-93.

468 [40] Y. Qiu, H. Ding, T. Su, Non-isothermal low-temperature reversible aging of commercial
469 wax-based warm mix asphalts, *International Journal of Pavement Engineering* 23(2) (2022)
470 514-522.

471 [41] H.A. Tabatabaee, R. Velasquez, H.U. Bahia, Modeling Thermal Stress in Asphalt Mixtures
472 Undergoing Glass Transition and Physical Hardening, *Transportation Research Record* (2296)
473 (2012) 106-114.

474 [42] H. Ding, Y. Qiu, A. Rahman, W. Wang, Low-temperature reversible aging properties of
475 coal liquefaction residue modified asphalt, *Materials and Structures* 51(3) (2018) 1-11.

476 [43] H. Wei, H. Zhang, J. Li, J. Zheng, J. Ren, Effect of loading rate on failure characteristics

477 of asphalt mixtures using acoustic emission technique, *Construction and Building Materials*
478 364 (2023) 129835.

479 [44] J. Zhu, X. Lu, R. Balieu, N. Kringos, Modelling and numerical simulation of phase
480 separation in polymer modified bitumen by phase-field method, *Materials & Design* 107 (2016)
481 322-332.

482 [45] J. Zhu, X. Lu, N. Kringos, Experimental investigation on storage stability and phase
483 separation behaviour of polymer-modified bitumen, *International Journal of Pavement*
484 *Engineering* 19(9) (2018) 832-841.

485 [46] Y. Lei, S. Han, J. Zhang, Effect of the dispersion degree of asphaltene on wax deposition
486 in crude oil under static conditions, *Fuel Processing Technology* 146 (2016) 20-28.

487 [47] P. Claudy, J. Letoffe, G. King, J. Plancke, Characterization of asphalts cements by
488 thermomicroscopy and differential scanning calorimetry: correlation to classic physical
489 properties, *Fuel Science & Technology International* 10(4-6) (1992) 735-765.

490 [48] H. Ding, H. Zhang, H. Zhang, D. Liu, Y. Qiu, A. Hussain, Separation of wax fraction in
491 asphalt binder by an improved method and determination of its molecular structure, *Fuel* 322
492 (2022) 124081.

493 [49] P.K. Das, H. Baaj, S. Tighe, N. Kringos, Atomic force microscopy to investigate asphalt
494 binders: A state-of-the-art review, *Road Materials and Pavement Design* 17(3) (2016) 693-718.

495